

## VISUALISATION OF CH, NO AND OH 2D-LIF IMAGES AND CONCENTRATION PROFILES PRODUCED IN LOW NO<sub>x</sub> BURNERS

D. PROCTOR, I.G. PEARSON and S. BRUMALE

CSIRO Division of Building, Construction & Engineering  
PO Box 56, Highett, VIC 3190, AUSTRALIA

### ABSTRACT

When investigating combustion zones in new types of combustors, it is often desirable to be able to look at where a particular molecular species is at a given point in time and space. CSIRO Division of Building, Construction & Engineering has been involved in investigating the mechanisms of low NO<sub>x</sub> and pulsating burners, using methane as the fuel source, with the prime aim of reducing greenhouse gas emissions from the combustion of CH<sub>4</sub>.

The principal species which are normally used to delineate where chemical reactions are taking place in combustion are CH and OH. 2-Dimensional Laser Induced Fluorescence images of these species as well as that of NO taken in a low NO<sub>x</sub> mesh burner, at an equivalence ratio of  $\phi = 0.9$ , are compared along with relative concentration profiles of these three species. The NO concentration profile indicates that there is a weak Zeldovich mechanism taking place in one part of the burner and a "prompt" mechanism in another zone.

### INTRODUCTION

At the CSIRO Division of Building, Construction & Engineering, we have put together a number of techniques to map the temperature and concentration of various molecular species within natural gas burners, and in particular the NO<sub>x</sub> emissions. As one of the major components in photochemical smog reactions, control of NO emissions in combustion processes is becoming more important. Concern about atmospheric pollution is leading to stricter control of emissions, requiring minimization of NO<sub>x</sub> production in flames.

Laser based species imaging, has many advantages in the combustion environment. It offers non-intrusive methods for measuring concentration and temperature, unlike the traditional methods of gas sampling or thermocouples. Laser methods can often also offer planar rather than point to point measurements, allowing more complete information about the flow field. Most of these laser based techniques have been developed under ideal conditions, but in the set of experiments described in this paper the techniques are being applied at close to their limits, particularly for the NO molecule.

### LASER INDUCED FLUORESCENCE TECHNIQUES

Laser Induced Fluorescence (LIF) techniques use the great intensity and mono-chromaticity of laser excitation to pump large numbers of molecules into a selected upper

state. This is achieved by tuning the laser to the wavelength of a particular transition of the molecule under investigation. These molecules relax, emitting fluorescence. By selecting a suitable transition, the properties of that transition can be used to investigate various properties of the molecule. For instance, if a temperature insensitive line is excited, the fluorescence signal can be used to measure concentration through various temperature regions of a flame. In a similar way the use of a temperature sensitive line can be used with known concentration to view the temperature field of a flame.

There are two possible fluorescence methods which can be used. A conditional averaged 2D-LIF approach to gain some indication of spatial molecular distribution, in this case of CH, NO and OH, and a LSF method to obtain single point, single shot concentration measurements. Only the first method was used in this work. In 2D-LIF measurements, one obtains an accumulated two dimensional fluorescence profile that can be related to concentration. The fluorescence signal detected relies on many factors. The number of molecules actually excited to the upper state depends on how many reside in the lower state, the intensity of the laser and the probability of the transition. The fraction of these fluorescing relies on the the number undergoing stimulated emission, the rate of spontaneous fluorescence, the quenching rate and the efficiency of the detection optics. Cattolica *et.al.*(1988) give a derivation and subsequent formula for the fluorescence signal.

This model makes various assumptions about the fluorescence, the validity of which must be considered for each experiment. The first assumption is that the system being modeled is essentially two leveled and the combined population of the upper level,  $N_2$  and the lower level,  $N_1$  is constant. The second assumption is that the laser excitation is in the unsaturated limit or more simply that the rate of absorption and stimulated emission is much lower than the combined rate of fluorescence and quenching. It can then be derived that nearly all the population resides in the lower state  $N_1$ .

The fact that this method occurs in the unsaturated limit means that few molecules actually make the transition to the upper state and of these only a small fraction fluoresce. This lends itself to time averaged or conditional averaged 2D-LIF measurements. If the quenching rate is high the fraction fluorescing is very small and the signal to noise ratio can become prohibitively large. In atmospheric flames the ambient pressure increases the quenching rate greatly and consequently high laser powers are required to achieve reasonable signal to noise ratios. This may force the excitation out of the unsaturated limit.

## EXPERIMENT

The excitation source for the experimental setup was a frequency doubled excimer, (Questek 2340 $\beta$  Excimer 308nm laser), pumped dye laser, (Quanta Ray PDL-3) with wavelength extender, WEX, using BBO crystals, which allowed the generation of a tunable light source in the desired excitation band. This laser source was formed into thin sheet, passed through the flame region and viewed at right angles to the beam. This allowed the viewing of a plane of the fluorescence.

CH laser induced fluorescence was observed by exciting the 427.4nm rotational line in the  $A^2\Delta(v' = 0) \leftarrow X^2\Pi(v'' = 0)$  with the fluorescence viewed at the same wavelength. In the case of OH, the transition used was the the  $Q_1(7)$  at 308.9734nm (Stepowski *et.al.*(1981)) in the  $A^2\Sigma^+(v' = 0) \leftarrow X^2\Pi(v'' = 0)$  transition band. The laser induced fluorescence was at the same wavelength.

For the case of NO, the transition pumped was  $A^2\Sigma^+(v' = 0) \leftarrow X^2\Pi_{1/2}(v'' = 0)$  at 225nm, which was obtained by doubling the same dye laser used to produce the CH fluorescence. The NO fluorescence was viewed at the  $A^2\Sigma^+(v' = 0) \rightarrow X^2\Pi_{1/2}(v'' = 2)$  band at 258nm. The line width of laser radiation was  $0.84\text{cm}^{-1}$ .

Suitable UV-optics and angle tuned 10nm narrow band pass filters were employed to collect the desired signal, free of reflected light. A description of the image capturing procedure is given elsewhere (Pearson *et.al.*(1991), Proctor *et.al.*(1991)). Accumulation of the result of single laser shot signals, with the removal of background noise and correction for optical distortion (Cruyningen *et.al.*(1991)), then produced in this case, as shown in Figure 1, for CH, OH and NO a time averaged plane image of the fluorescence signal which may then be related to species number density. An intensified gated CID camera, (ITT F4573-111123), with a 5ns gate, was used to capture the fluorescence signal since it provided a better signal to noise ratio by ensuring the signal was read when the peak power of the desired fluorescence occurred and also greatly reduced the effect of collisional quenching on the induced fluorescence signal.

The burner which was used in this experiment was a low  $\text{NO}_x$  design produced by Bowin for use in un-flued environments. It consists of a series of metal meshes, not unlike that shown in Figure 1 of Golombok *et.al.*(1991) except that it is not a sintered metal like their Shell burner. An external view is shown in Figure 2 and is the view seen by the intensified camera. As can be seen from this figure, the burner is of the "flameless" type.

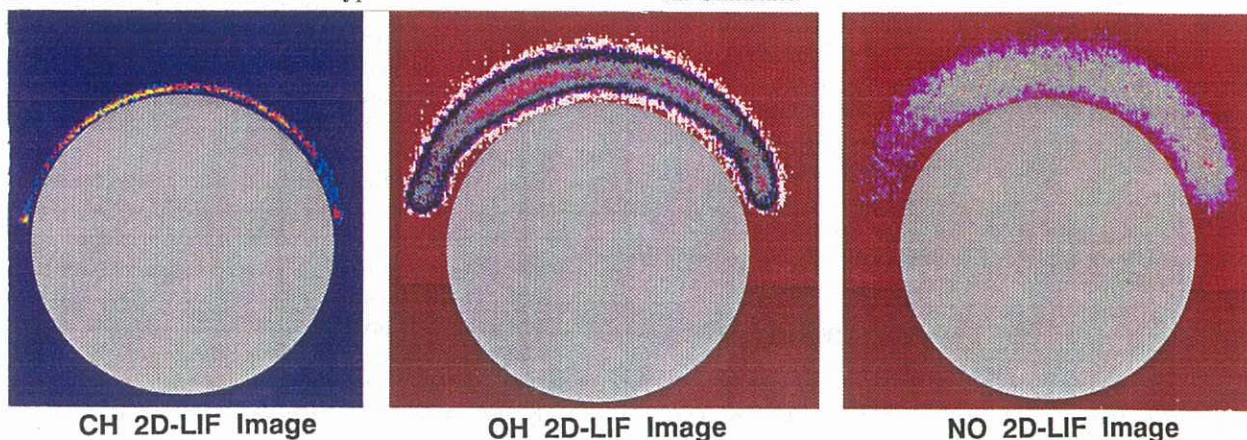


Figure 1: CH, OH and NO concentrations in a low  $\text{NO}_x$  burner.

## RESULTS

Besides correcting for the effects of quenching and background noise, the intensity of the images were also corrected for the non-linearities in quantum efficiency as a function of wavelength, and the CID camera gain.

Radial concentration profiles of each of the three species measured were obtained, one of which is shown in Figure 3. The basic shape of each set of CH and OH profile is almost identical, except for the absolute maximum values and the radial position at which they occur. This is reflected in the shape of the NO profile, where the maximum appears further out but always immediately after the OH peak.

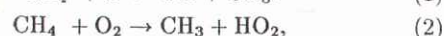
### CH profile.

The CH radical exists in a very thin layer and is a consequence of the production from two reactions, whose reactants are both produced at the same time<sup>1</sup>. Both these CH producing reactions are proceeding at almost the same rates at the temperature existing, ( $1080\text{K}\pm 2$ ), in the region adjacent to the mesh where the CH was being formed. This very thin shell is similar to that found by Norton and Smyth(1991), who note that it is one of the thinnest images that they have seen.

The removal of the CH radical is confined to 12 reactions, some of which provide reactants for the production of NO and OH as well as the removal of these species. In this particular burner, the temperature in the CH removal region is  $\sim 1080\text{K}$ , and consequently the removal reactions are all progressing at virtually the same rate. This could be the reason for the rapid demise of the CH radical shown in Figure 3.

### OH profile.

OH on the other hand, can be produced from many reactions, which can be considered as occurring as a chain of reactions or in five possible waves, each with a number of possible reactions. It can be seen from Figure 3, that in the Bowin burner, the OH has the highest concentration of the three species OH, CH and NO, close to the burner mesh. This follows from the initial reaction taking place which is the oxidation of  $\text{CH}_4$  and the formation of NO reactions:



<sup>1</sup>Due to space limitations, the 85 CH, OH and NO production and removal chemical reactions are not listed, but will be presented at the Conference.

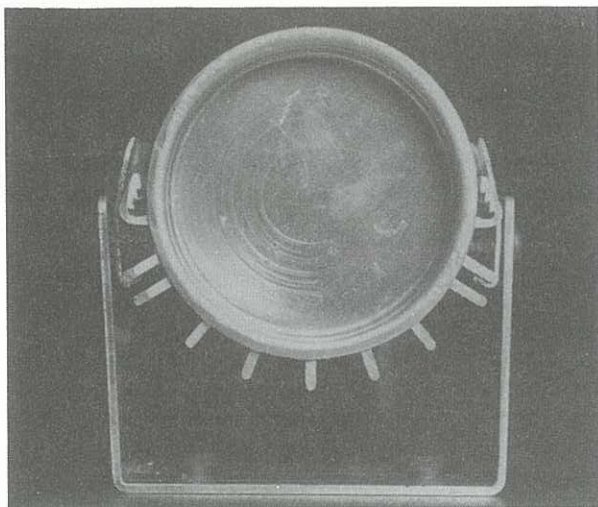


Figure 2: End view of Bowin mesh burner, (lit), as seen by species imaging camera.

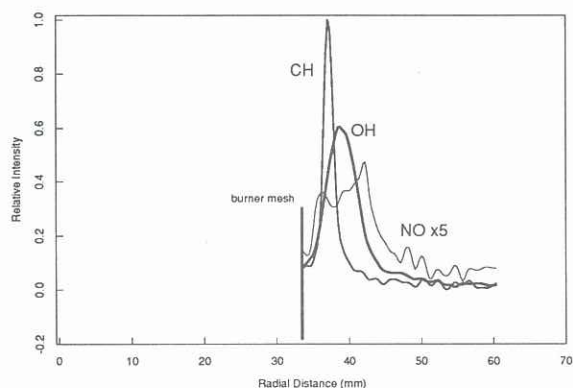


Figure 3: Relative CH, NO and OH concentration profiles in a low  $\text{NO}_x$  burner.

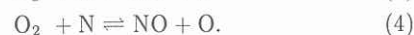
which produce the necessary radicals for the subsequent rapid production of OH, before the  $\text{CH}_2$  reactants necessary for the production of CH is formed. The second OH producing wave consists of the production of  $\text{CH}_3\text{O}$ , which leads to the third wave set of possible reactions with the production of  $\text{CH}_2\text{O}$ , which together with  $\text{CH}_2$  leads to the fourth wave and the first stage in the "Prompt" NO mechanism.

The fourth wave of reactions consists not only of the  $\text{CH}_2/\text{CH}_2\text{O}$  reactions but also the NO removal before the CH peak, which is consistent with the dip in the NO profile at a radial position of 36mm. The reactant products from the fourth wave reactions, i.e. HCN, HCO and CO, also provide the reactants for the "Prompt" NO production. The removal of OH is equally as complex and occurs in a set of chain reactions some of which produce either CH or NO or the reactants necessary to produce more OH. This latter effect leads to a spreading out of the OH profile as well as causing it to tail off. It should be borne in mind, that the species concentrations will appear to decrease quicker due to radial nature of the burner. The reactions sets that are considered to be taking place are as follows. Firstly, those that occur before the CH radical appears and ending with the appearance of CH,  $\text{H}_2\text{O}$  and H. The next set of reactions probably are occurring simultaneously and require the products from the first set of removal reactions. They lead to the removal of CH as well, forming HCO,  $\text{H}_2\text{O}$  and

H. The HCO then reacts with the OH to produce CO and  $\text{H}_2\text{O}$ . And lastly, there are a group of reactions, three of which are contributing to the NO concentration through minor "Prompt" mechanism routes.

#### NO profile.

The NO production and subsequent removal appears to be much more complex since there are reactions which remove NO between production peaks. The main NO peaks appear to be from five distinct sets of reactions producing NO interspersed with some faster removal steps. The first group occurs right at the burner mesh and consists of the Zeldovich thermal  $\text{NO}_x$  mechanism. This is despite the fact that the temperature at the burner mesh is only  $1136\text{K} \pm 2$ , which is close to that predicted by Golombok *et al.*(1991). It would appear that mesh burners operate like catalytic burners or, the other possibility exists that catalytic burners are operating like mesh burners(Shirvill(1991)):



Sathe *et al.*(1990) and Tong *et al.*(1990) have analysed a porous matrix burner, which was similar in concept to the Shell sintered metal mesh(Golombok *et al.*(1991)), except that the former were dealing with a ceramic fibre. This type of burner is virtually identical to the Alzeta<sup>®</sup>(Schreiber *et al.*(1983)) burner, which is promoted as a catalytic burner. The following reactions can also possibly take place, since the necessary radicals are also present close to the mesh from the initial oxidation of  $\text{CH}_4$ :



This last reaction can also occur later on and can lead to another two NO peaks. The first is the main "Prompt" route and is dealt with separately below. The other will happen after the OH peak and after the next two reactions, which require the products from the CH removal reactions to begin the sequence after the formation of CH and its removal. The reasoning behind this is that N radicals can also be produced at this time from reactions involving removal of OH.



It is doubtful if the last reaction is taking place if the HNO is being produced from  $\text{CH}_2$  and  $\text{N}_2$  via the steps based on Miller and Bowman(1989). There is another route to HNO. It is thought that reaction (8) is not a single step reaction and occurs through two intermediate steps, one of the products being HNO, via the removal of OH with N to produce first HON, then HNO.

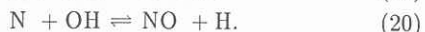
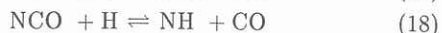
The main "Prompt" route to NO starts with either the formation of CN and N radicals via



or reaction (16) according to Fenimore(1971):



followed by a series of rapid chain reactions (Miller *et al.*(1985)) terminating with reaction (8) above:



Coupled with the last 5 reactions are a set of recycling reactions involving C, CH and the singlet and triplet states  $^1\text{CH}_2$  and  $^3\text{CH}_2$  in the removal of NO, favoured under fuel rich conditions. (NB. It should be noted that the reverse of reaction (15) is very fast (Slack(1976), Natarajan(1986)), even at room temperature (Whyte(1983)) and thus reaction (15) is a less likely route to "Prompt" NO.)

Removal of NO has in part already been dealt with, but the reaction will be included here. The first is the reverse of reaction (3) and can lead to the first dip in the NO concentration profile just after the first peak:



Some of the above reactions can commence again after the CH peak, once reactions have stopped producing the N radical. The next group of reactions are those involving the  $\text{CH}_2$  radical, the first of which is one of the "Prompt" recycle mentioned above. The  $^1\text{CH}_2$  state tends to be more reactive than the  $^3\text{CH}_2$  state (Miller & Bowman(1989)). (Those involving  $\text{CH}_3$  have been neglected since they are too slow, particularly in the Bowin burner, in which the temperatures are much lower than conventional burners.):



Whilst the above two reactions are taking place, CH is also being formed. This then provides the next reactant for the next removal mechanism for NO, the one being another of the "Prompt" recycle reactions:



which create a dip in the NO concentration between the CH peak and the OH peak if the removal rate is faster than the production rate. The last removal reactions are the reverse reaction of reaction (8) above and the formation of  $\text{N}_2\text{O}$ .



Although the NH radical has been included in some of the steps above, it is thought that it is very unlikely to be occurring in the "flame" of this mesh burner. Similarly with CN, and it is the reason that reactions involving these two species have been in the main neglected.

## CONCLUSIONS

Three images of important molecular species, namely CH, NO and OH, in an atmospheric pressure, low  $\text{NO}_x$ , natural gas combustor have been obtained to gain important information about the concentration distributions and hence reactions taking place.

Despite the complexities of the NO reactions, a fairly clear picture of what is taking place in this burner is presented. The OH picture is somewhat partially unresolved, as the processes are smeared out due to earlier reactions in the chain of events being able to recommence.

One of the several unresolved questions remaining is that pertaining to whether this type of burner belongs to the porous class or the catalytic class of burner. It may be that both the catalytic and porous types of burners are functioning under both mechanisms simultaneously.

## ACKNOWLEDGEMENT

Part of this work was supported by a grant from the NSW Department of Minerals and Energy, and assistance from AGL and Bowin Design.

## REFERENCES

- Catollica R. J., Cavolowsky J. A. & Mataga T. G. (1988) **22<sup>nd</sup> Symp. (Int.) on Combustion**. Uni. Washington, Seattle, Aug 14-19.
- Cruyningen, I., Lozano, A. & Hanson, R.K. (1991) **Experiments in Fluids** **10** 40-49.
- Fenimore, C.P. (1971) *13<sup>th</sup> Int. Symp. on Combustion* pp 373-379, Combustion Inst., Pittsburgh.
- Golombok, M., Prothero, A., Shirvill, L.C. & Small, L.M. (1991) **Combust. Sci. and Tech** **77** 203-223.
- Miller, J.A. & Bowman, C.T. (1989) **Prog. Energy Combust. Sci.** **15** 287-338.
- Miller, J.A.; Branch, M.C.; M<sup>c</sup>Lean, W.J.; Chandler, D.W.; Smooke, M.D. & Kee, R.J. (1985) *20<sup>th</sup> Int. Symp. on Combustion*, pp673-684, Combustion Inst., Pittsburgh.
- Natarajan, K. & Roth, P. (1986) *21<sup>st</sup> Int. Symp. on Combustion*, pp 729-737, Combustion Inst., Pittsburgh.
- Norton, T.S. & Smyth, K.C. (1991) **Combust. Sci. and Tech.** **76** 1-20.
- Pearson, I.G. & Proctor, D. (1991) *Proc. 2<sup>nd</sup> World Conf. on Experimental heat Transfer, Fluid Dynamics & Thermodynamics*, Dubrovnik, Yugoslavia, 23-28 June.
- Proctor, D., Pearson, I.G. & M<sup>c</sup>Leod, M. (1991) *1<sup>st</sup> International Conf. on Combustion Technologies for a Clean Environment*, Vilamoura, Portugal, 3-6 Sept.
- Sathe, S.B., Peck, R.E. & Tong, T.W. (1990) **Int. J. Heat Mass Transfer** **33** 1331-1338.
- Schreiber, R.; Krill, W.; Kesselring, J.; Vogt, R. & Lukasiewicz, M. (1983) *3<sup>rd</sup> Int. Gas. Res. Conf.*, Paper **IGRC/D06-83**.
- Shirvill, L.C. (1991) (Shell Research Ltd, Thornton, Cheshire, UK) *Personal Communication Sept.*
- Slack, M.W. (1976) *J. Chem. Phys.* **64**, 228.
- Stepowski D. & Cottureau M.J. (1981) **Combustion and Flame** **40** 65-70.
- Tong, T.W., Sathe, S.B. & Peck, R.E. (1990) **Int. J. Heat Mass Transfer** **33** 1339-1346.
- Whyte, A.R. & Phillips, L.F. (1983) *Chem. Phys. Lett.* **98**, 590.